

## Fabrication of circular optical structures with a 20 nm minimum feature size using nanoimprint lithography

Mingtao Li,<sup>a)</sup> Jian Wang, Lei Zhuang, and Stephen Y. Chou

*NanoStructure Laboratory, Department of Electrical Engineering, Princeton University, Princeton, New Jersey 08544*

(Received 12 October 1999; accepted for publication 10 December 1999)

We demonstrated the fabrication of Fresnel zone plates with a 75 nm minimum feature size and circular gratings with a 20 nm minimum linewidth in polymethyl methacrylate using nanoimprint lithography, and in metals by means of a lift-off technique. Observation of sharp Moiré patterns indicated the high fidelity of nanoimprint lithography in pattern duplication. Our results showed that nanoimprint lithography is a promising technology for patterning integrated optics. © 2000 American Institute of Physics. [S0003-6951(00)03906-1]

Nanoscale circular patterns such as zone plates and optical couplers with circular gratings<sup>1,2</sup> are key elements in integrated optics, optical interconnects, beam focusing, and maskless lithography systems. Typically, nanoscale circular patterns were fabricated using electron-beam lithography<sup>3-7</sup> and x-ray lithography.<sup>8</sup> For mass production, however, a low-cost and high-throughput lithographic method is needed.

Nanoimprint lithography (NIL)<sup>9</sup> is emerging as an economical and high-throughput nanopatterning technology for nanostructure engineering. Previously, NIL has demonstrated 10-nm-diam dots and 15-nm-linewidth gratings.<sup>10</sup> However, until now it was not clear whether NIL can pattern nanoscale circular concentric structures with high fidelity. In this letter, we present the fabrication of nanoscale circular gratings and Fresnel zone plates with high precision by nanoimprint lithography and a lift-off technique.

The circular gratings we fabricated consist of concentric rings with radii equal to an integral multiple of the smallest ring radius (i.e., the pitch), which was chosen to be 100 and 150 nm in our experiment. The Fresnel zone plates (FZP) we fabricated were composed of concentric circles with their radii proportional to the square root of integers times the wavelength. The space between two adjacent circles was defined as one zone. The alternating transparent and opaque zones (with respect to the incident irradiation) allow the FZPs to act as a lens. Due to a limited single writing field of our electron-beam lithographic system, the FZPs designed were composed of 50 zones, with a diameter of 15 and 25  $\mu\text{m}$ , respectively. Hence, the minimum linewidth and the focal length for an x ray with a 1 nm wavelength were 75 nm and 0.1125 cm, and 125 nm and 0.3125 cm, respectively.

The first step in fabrication was to make imprint molds using electron-beam lithography. Zone plates and circular gratings were delineated on a layer of 70-nm-thick 950 000 molecular weight polymethyl methacrylate (PMMA) spun on a silicon substrate with thermal oxide. After development in a cellosolve/methanol developer, the exposed patterns were transferred to chromium (Cr) by evaporation of Cr and a lift-off in heated acetone. Ultrasonic agitation was used in the lift-off procedure. Reactive ion etching (RIE) with

$\text{CHF}_3/\text{O}_2$  chemistry was then used to transfer the metal patterns into the oxide. The chromium mask was subsequently stripped off in chromium etchant (CR-7). The protrusion on the mold is approximately 100 nm high. Single circular gratings and a circular grating array were patterned on one mold. Zone plates were fabricated on a separate mold.

The molds were used to pattern PMMA on silicon substrates, and PMMA patterns were later transferred to metals (Cr/Au) by lift-off. Chromium serves as an adhesion layer, and gold (Au) is suitable for inspection by scanning electron microscope (SEM). Figure 1 shows a schematic of the fabrication procedure of circular rings and FZPs by nanoimprint lithography. The imprint resist was a layer of 120-nm-thick 15 000 molecular weight polymethyl methacrylate spun on a silicon substrate. The imprint temperature and pressure were 175 °C and 645 psi, respectively. A parallel-plate imprint machine was used. The mold and the imprinted sample were

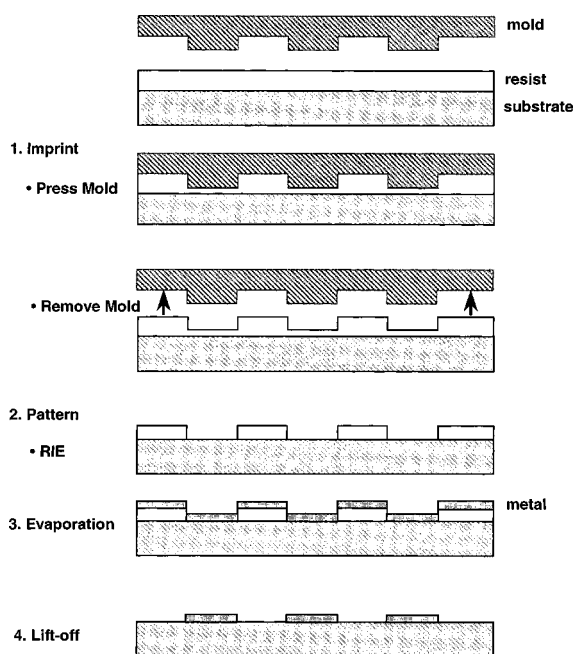


FIG. 1. Schematic of nanoimprint lithography: (1) imprint using a mold to create a thickness contrast in PMMA, then separate the mold from the substrate; (2) pattern transfer down to PMMA through anisotropic oxygen etching to remove the residual PMMA in the compressed area; (3) metal deposition; and (4) lift-off in warm acetone.

<sup>a)</sup>Author to whom correspondence should be addressed; electronic mail: mtl@ee.princeton.edu

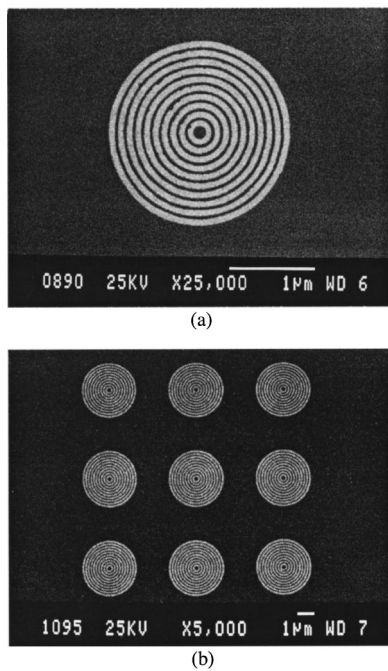


FIG. 2. (a) Circular concentric gratings with a period of 100 nm, and (b) an array consisting of circular gratings with a 150 nm period, fabricated by nanoimprint lithography and lift-off. The linewidths are (a) 80 nm and (b) 90 nm, respectively.

separated manually. Detailed descriptions of nanoimprint lithography have been presented elsewhere.<sup>9</sup>

Figure 2 shows nanoscale, metallic, circular gratings with periods of 100 and 150 nm fabricated on a silicon substrate by NIL and lift-off. A spacing as close as 20 nm between metal ridges was achieved. The linewidth reduction during oxygen etching was less than 10%,<sup>11</sup> which means that rings with a 20 nm linewidth were imprinted in PMMA.

Figure 3 shows a Fresnel zone plate with a 75 nm minimum linewidth and total diameter of 15  $\mu\text{m}$  imprinted into PMMA film. A tapping-mode atomic force microscope (AFM) was employed to inspect the surface topology of the PMMA template. The PMMA arcs are very smooth, indicating excellent conformity of the PMMA to the mold. After oxygen RIE to remove the residual PMMA at the trench bottom and deposition of metals by electron-beam evaporator, the metals (Cr/Au) were lifted off in warm acetone. Figure 4 shows the metallic zone plates with a 125 nm minimum linewidth and 25  $\mu\text{m}$  diam. Both positive and negative tone zone plates were fabricated.

Moiré fringes offer an effective method to examine the pattern inaccuracies of FZP.<sup>12</sup> They were investigated qualitatively by a superposition of two images of the positive FZP, as described in Fig. 5. The Moiré fringes inspected are perpendicular to the shifting direction [Fig. 5(a)], and no fringes are observed for two overlapped images when one is being rotated 90° and 180° relative to the other [Figs. 5(b) and 5(c)]. Compared with the simulation results given by Vladmirsky,<sup>12</sup> our results indicate the absence of ellipticity, radial displacement, and nonconcentricity of zones, thereby showing a high pattern transfer fidelity and excellent control of the accurate linewidth and zone spacing. The fidelity of pattern duplication is attributed to the accurate definition of patterns by electron-beam lithography and highly anisotropic pattern transfer by fluorine-based and oxygen reactive ion

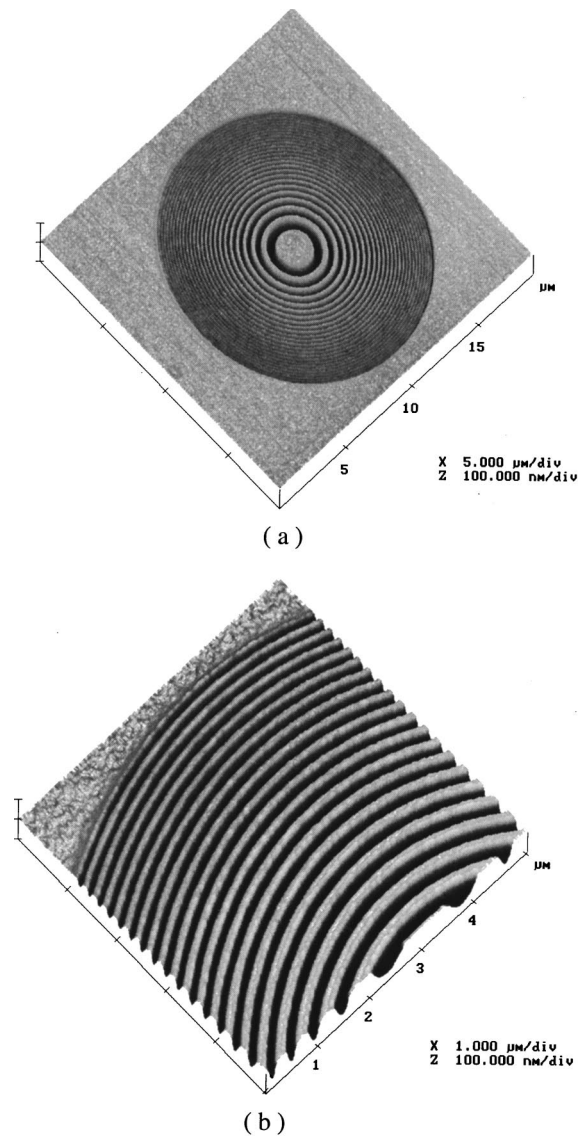
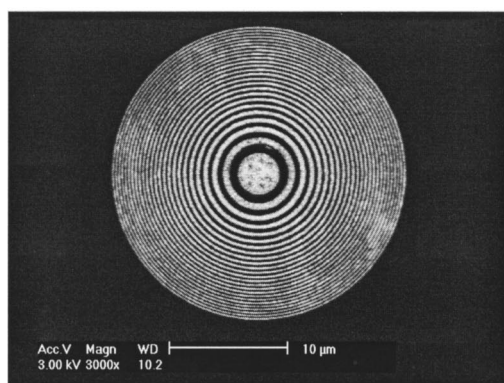


FIG. 3. AFM images of PMMA zone plates with a minimum linewidth of 75 nm and 15  $\mu\text{m}$  in diameter, made by nanoimprint lithography. (b) is a detailed partial section of (a).

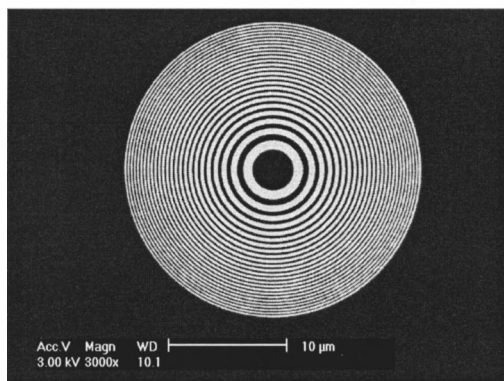
etching. It is also due to the good surface properties of molds, which were treated by a fluorinated surfactant to reduce their surface energy to make them dewet PMMA.

We have found that air bubbles can be eliminated during fabrication by an appropriate selection of both PMMA thickness and imprint conditions. At thermodynamic equilibrium, the solubility of air in PMMA depends on both temperature and pressure. Air dissolves in PMMA by occupying free-volume sites or interstitial sites to form bonds with the PMMA molecules.<sup>13</sup> Other factors like moisture and solvent (chlorobenzene) might also contribute to the formation of air bubbles. A prebake of PMMA film and imprint under vacuum obviously help to eliminate air bubbles. With a proper imprint pressure, air remaining in the volume confined by the mold and the PMMA film has no obvious negative effects on pattern duplication, as shown by our experiment. The depth of the trenches duplicated in PMMA is uniform across the entire sample surface, although about 5% shallower than the protrusion height on mold.

Finally, we found that low molecular weight PMMA, above its glass transition temperature, has excellent flow



(a)



(b)

FIG. 4. SEM images of metallic zone plates with  $25\ \mu\text{m}$  diam and  $125\ \text{nm}$  minimum linewidth, fabricated by nanoimprint lithography and lift-off. (a) Positive tone and (b) negative tone zone plates are fabricated simultaneously.

characteristics to satisfy the needs of NIL. For example, a Fresnel zone plate is a diffraction grating with a line density gradually increasing from the center. The mass transport of PMMA under pressure is different in the vicinity of different sized features on the mold when the mold is pressed into the PMMA film. Under suitable pressure and temperature, PMMA flows sufficiently to conform to the mold. Hence, zone plates on the mold surface can be transferred into PMMA with high fidelity.

In conclusion, nanoimprint lithography is capable of patterning nanoscale circular structures with controlled linewidth. Air bubbles can be eliminated under proper processing conditions, and PMMA flows adequately to conform to different features on the mold. Optical elements can be made with low cost and high throughput. Nanoimprint lithography will have many applications in the fabrication of integrated optics.

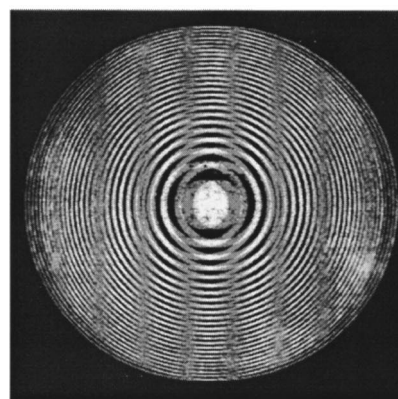
<sup>1</sup>M. Fallahi, K. J. Kasunic, S. Penner, O. Nordman, and N. Peyghambarian, *Opt. Eng. (Bellingham)* **37**, 1169 (1998).

<sup>2</sup>C. M. Wu, M. Svilans, M. Fallahi, I. Templeton, T. Makino, J. Glinski, R. Maciejko, S. I. Najafi, C. Blaauw, C. Maritan, and D. G. Knight, *IEEE Photonics Technol. Lett.* **4**, 960 (1992).

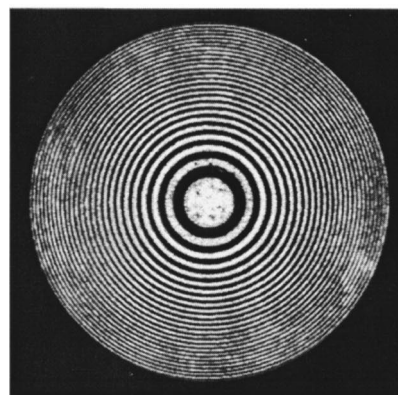
<sup>3</sup>T. Erdogan, O. King, G. W. Wicks, D. G. Hall, E. H. Anderson, and M. J. Rooks, *Appl. Phys. Lett.* **60**, 1921 (1992).

<sup>4</sup>O. King, T. Erdogan, G. W. Wicks, D. G. Hall, E. H. Anderson, D. Costello, and M. J. Rooks, *J. Vac. Sci. Technol. B* **10**, 2974 (1992).

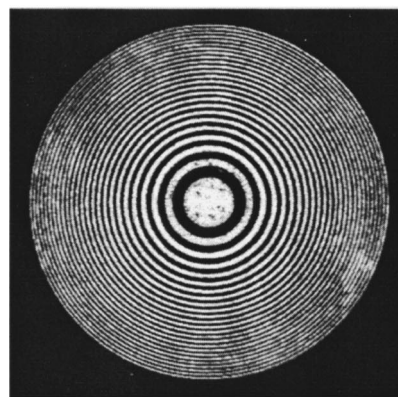
<sup>5</sup>G. Schneider, T. Schliebe, and H. Aschoff, *J. Vac. Sci. Technol. B* **13**, 2809 (1995).



(a)



(b)



(c)

FIG. 5. Investigation of Moiré fringes by a superposition of two images of FZP. (a) Obtained by a shift of two SEM images; (b) a superposition of two images rotated  $90^\circ$  relative to each other without a shift; and (c) a superposition of two images rotated  $180^\circ$  relative to each other without a shift.

<sup>6</sup>J. R. Wendt, G. A. Vawter, R. E. Smith, and M. E. Warren, *J. Vac. Sci. Technol. B* **15**, 2946 (1997).

<sup>7</sup>Y. Vladimirovsky, D. Kern, T. H. P. Chang, D. Attwood, H. Ade, J. Kirz, I. McNulty, H. Rarback, and D. Shu, *J. Vac. Sci. Technol. B* **6**, 311 (1988).

<sup>8</sup>A. Ozawa, T. Tamamura, T. Ishii, H. Yoshihara, and T. Kagoshima, *Microelectron. Eng.* **35**, 525 (1997).

<sup>9</sup>S. Y. Chou, P. R. Krauss, and P. J. Renstrom, *Appl. Phys. Lett.* **67**, 3114 (1995); *Science* **272**, 85 (1996).

<sup>10</sup>S. Y. Chou and P. R. Krauss, *Microelectron. Eng.* **35**, 237 (1997).

<sup>11</sup>P. Krauss, Ph.D. thesis, University of Minnesota (1997).

<sup>12</sup>Y. Vladimirovsky and H. W. P. Koops, *J. Vac. Sci. Technol. B* **6**, 2142 (1988).

<sup>13</sup>J. F. Stevenson, *Innovation in Polymer Processing: Molding* (Hanser/Gardner, Cincinnati, OH, 1996), Chap. 3, p. 109.